ACS Sustainable Chemistry & Engineering

Research Article

pubs.acs.org/journal/ascecg

Ag@AgCl Nanomaterial Synthesis Using Sugar Cane Juice and Its Application in Degradation of Azo Dyes

Anand A. Kulkarni and Bhalchandra M. Bhanage*

Department of Chemistry, Institute of Chemical Technology, Matunga, Mumbai 400 019, India

Supporting Information

ABSTRACT: This work reports on an additive-free method for the preparation of hybrid Ag@AgCl plasmonic nanoparticles (NPs) with a size less than 50 nm (average size 37 nm) using sugar cane juice as the only reagent for the first time. This is an ecofriendly, rapid (20 min), and economical protocol that avoids the use of additional external reducing agents, external capping agents, templates, solvents, and external halide ion sources. The effects of various parameters like the concentration of sugar juice, reaction temperature, and reaction time on the formation of Ag@AgCl with respect to morphology control and size distribution were also studied. The prepared NPs were well characterized using techniques such as FEG-SEM, XRD, TEM, XPS, UV−visible spectrometry, and EDS. Prepared Ag@AgCl nanomaterials exhibited good photocatalytic ability toward degradation of methyl orange and methylene blue azo dyes in aqueous solution in the visible region of light. The catalyst was tested up to four recycles and showed no significant loss of catalytic activity.

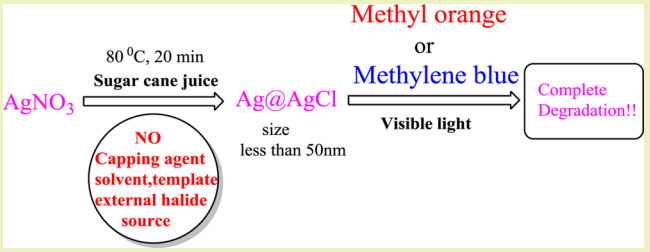

KEYWORDS: *Green chemistry, Nanoparticles, Silver, Phytosynthesis, Photocatalyst*

INTRODUCTION

Nanobiotechnology represents the intersection of nanotechnology and biotechnology, which is an emerging field dedicated to the creation, improvement, and utility of nanoscale structures for advanced biotechnology.[1] The nanomaterials are prepared by using various physical and chemical methods; however, most of these methods are energy and capital intensive. The conventional methods involve the use of capping agents, toxic solvents, harsh chemicals, and other additives, limiting their use in biomedical and clinical fields. Developing a greener protocol for chemical synthesis that avoids the use of solvents and stoichiometric reagents, aviods waste byproducts, and utilizes available renewable resources is a need of the chemical industry. Several efforts have been devoted toward biosynthesis of metal nanoparticles using bacteria,[2] fungi,[3] actinomycetes,[4] yeast,[5] and viruses.[6] In addition to the above-mentioned methods of preparation, a new method that uses the part of whole plant for the synthesis of NPs known as phytosynthesis is under development and is an advantageous and profitable approach. The phytosynthesis of noble metal nanoparticles (Ag, Pd, Pt, and Au) has gained significant attention in the past decade[7−9] because of the its use in catalysis, drug delivery, biomedical sensors, etc. In comparison to methods involving the use of microorganism, phytosynthesis is a rapid and cost-effective approach that can be easily scaled up for bulk production of nanoparticles.[10] The phytosynthesis of nanoparticles will have more significance if the prepared nanoparticles are uniform in size and shape and are well dispersed. So, there is considerable scope for the new protocols based on use of plant extract for preparation of new nanomaterials with added advantages over routine chemical and physical methods.

Saccharum officinarum (sugar cane) is the crop that belongs to poaceae family. They have stout jointed fibrous stalks that are rich in sugar that is mainly accumulated at internodes. The juice extracted from sugar cane (sugar cane juice) is a mixture of reducing (glucose) as well as nonreducing sugars (sucrose), organic acids such as malic acid, oxalic acid, citric acid, succinic acid, and D-gluconic acid, and inorganic ions such as chloride, calcium, sodium, etc.[11−13] (Table S1, Supporting Information). Therefore, we reasoned that sugar cane juice is a bag full of reducing agents (glucose), well-known capping agents (organic acids), and halide ion sources (chloride ion) that can be utilized for preparation of nanomaterials.

The development of novel photocatalytic nanomaterials has gained significant importance for their application in various photocatalytic reactions, particularly for degradation of organic pollutants in air or solution.[14] Such heterogeneous photocatalysts work by absorbing photon energy from light and using it for chemical conversion. The best photocatalyst is the one that can work under normal sunlight for its practical application, and it can be attained by the surface modification of the photocatalyst to perform in the visible region of light. Various techniques such as doping with metallic elements[15] or nonmetallic elements[16] and anchoring organic dye molecules on the surface of photocatalyst[17] are reported to modify the

Received: December 31, 2013
Revised: February 13, 2014
Published: February 25, 2014

surface of the photocatalyst to cause them to absorb in the visible region of light. In these various techniques, surface modification by doping of noble metals is becoming more popular. However, most of the reported studies are confined to the doping of silver and gold metals. Several efforts have been devoted in this field to develop such silver- or gold-doped photocatalyst.[18−22]

The survey of literature revealed that the immobilization of noble metal NPs such as silver or gold on the surface of the photocatalyst leads to absorption of light in the visible region. In these lists of photocatalysts, the surface modification of the silver chloride (AgCl) photocatalyst by doping the silver metals on the surface of AgCl (referred as Ag@AgCl) has attracted the attention of many researchers because of the use of AgCl in the degradation of azo dyes such as methyl orange and methylene blue. The AgCl alone does not have the ability to absorb light in the visible region of sunlight, limiting its use in the practical application for degradation of dyes that are considered as pollutants in water. But when Ag metal is doped on the surface of AgCl, the AgCl starts to absorb light in the visible region of sunlight making it a useful photocatalyst for practical applications in the degradation of dyes. Huang and co-workers demonstrated the synthesis of Ag@AgX (X═Cl, Br) using an ion exchange reaction between the aqueous solution of Ag_2MoO_4 and HX followed by conversion of Ag^+ ions to Ag^0 under UV irradiation.[23−26] The prepared Ag/AgX is highly efficient and stable, but the approach has several limitations such as multistep synthesis and the use of expensive UV radiation techniques as well as a long reaction time. An et.al reported a facile synthesis of a sunlight-driven Ag:AgCl nano-sized photocatalyst.[19] Although the report highlighted the detailed description of Ag@AgCl preparation with selective morphology, characterization, and its application, the use of costly polymers such as PVP as a capping agent, variation in temperature from 100 to 150 °C during synthesis, size of the obtained catalyst greater than 100 nm (causing less surface area), and use of external halide source leads to some limitations for practical catalytic application. Varma et.al reported a green and clean methodology by using beet juice as the reducing and capping agents using microwave energy.[18] They obtained NPs of about 100 nm with uniform size, and they required an external source of the halide ion, i.e., NaCl for Ag@AgCl preparation. Other facile methodologies that were explored also have one or more drawbacks.[27−30] Recently Jang et.al reported on the low-temperature aqueous-phase synthesis of silver/silver chloride plasmonic nanoparticles with the size about 57 nm as visible light photocatalysts.[31] Similarly, Tang et.al also reported a facile large-scale synthesis route to form Ag@AgCl cubic cages with well-defined hollow interiors using a water-soluble sacrificial salt crystal template process.[32] In most of the above-reported methods, the synthesis of Ag@AgCl requires the use of a capping agent, external source of a halide ion, and a longer reaction time. The size of the obtained Ag@AgCl NPs in most of the reported methods is around 100 nm. For pollutant abatement application, the separation of additives (capping agents, stabilizers, and templates) is a difficult task for application on the bulk scale, and these additives also make the process economically unviable. As the prepared Ag@AgCl material is used as a photocatalyst, it is important to have more contact between the catalyst and pollutant adsorbed on them, which will be possible when the catalyst has greater surface area (smaller size of NPs). Thus, the surface area of the catalyst decides the overall catalytic efficiency. So, there is a considerable need for the development of more economically greener methods for Ag@AgCl NPs that involves good control on size and morphology without the use of capping agents, templates, solvents, and other additives.

Herein, an additive-free method for the preparation of hybrid Ag@AgCl plasmonic NPs with a size less than 50 nm (average size 37 nm) using sugar cane juice as the only reagent has been reported for the first time. Our investigation provides an environmentally benign synthetic route for preparation of Ag@AgCl NPs, and the method is simple, ecofriendly, fast (20 min), and economical. Additionally, the present protocol avoids the use of any external reducing agents, external capping agents, templates, solvents, and external halide ion sources. The present protocol not only overcomes the above demerits but also offers some additional features making the method greener. We have also studied the catalytic activity of these prepared Ag@AgCl NPs in the degradation of methylene blue (MB) and methyl orange (MO) dyes that are environmental pollutants in water.

EXPERIMENTAL SECTION

Material and Methods. Silver nitrate ($AgNO_3$), absolute ethanol, methylene blue (20 mg L^{-1}), and methyl orange (10 mg L^{-1}) were purchased from Sigma Aldrich, Ltd. All the chemicals were of analytical grade and were used without further purification/pretreatment. The deionized water distilled by a water purification system (Milli-Q) was used for washing. The sugar cane juice was obtained as per the method described below.

Preparation of Sugar Cane Juice. The locally purchased *Saccharum officinarum* (sugar cane) stems were crushed using the two roller crusher machine to extract the sugar cane juice. The crushing process breaks the hard nodes of the cane and flattens the stems. The juice was collected and filtered through a Whatmann filter paper no. 41 to remove the small fibers of sugar cane. No water was added during this process to avoid contamination of external ions.

Synthesis of Ag@AgCl Photocatalyst. In a typical synthesis, 1.5 mmol (254.80 mg) of $AgNO_3$ was dissolved in 30 mL of sugar cane juice in a 50 mL round-bottomed flask that resulted in formation of pale yellow-colored turbidity just after mixing. The reaction mixture was stirred vigorously on a hot plate at temperature of 80 °C for 20 min. After 20 min, the reaction mixture turned gray in color. The NPs of Ag@AgCl were separated by centrifugation, washed with double deionized water for four to five times for removing the adhered sugar juice followed by washing with absolute ethanol to remove adhered organic matter, and then dried in a vacuum oven at 50 °C.

Characterization of Materials. The X-ray diffractometer pattern of the prepared Ag@AgCl catalyst was obtained on a Shimadzu LabX XRD-6100 with the scan speed of 2°/min over a range from 20° to 90° using the copper target with λ = 1.54 Å. The transmission electron microscopy (TEM) images were recorded with a Phillips model CM 200 to study the morphology and size of the prepared NPs. Field emission gun-scanning electron microscopy (FEG-SEM) images were obtained using a TESCAN MIRA 3 model. The energy dispersive X-ray spectral analysis (EDS) image was recorded with an Oxford instrument at 10 kV and beam intensity of 15 to avoid the reduction of silver ion at higher voltage; beam intensity was kept high to get good response by the detector.

Evaluation of Photocatalytic Activity. Photocatalytic activity was studied by degrading the aqueous solution of MB and MO dyes. For this purpose, 100 mg of catalyst was mixed with 25 mL of MB dye (20 mg L^{-1} Aldrich) in a round-bottomed flask. The suspended solution was allowed to stand for 1 h in the dark to attend the adsorption−desorption equilibrium of dye on the surface of the catalyst before irradiation. The reaction mixture was then irradiated with a quartz halogen lamp that provided cold light free from the wavelength of UV region. After completion of the reaction, the catalyst was separated from the reaction mixture by centrifugation with RCF

18450 g. The UV−visible spectroscopy was used to study the degradation of dyes. The same procedure was applied for the MO dye (conc. 10 mg L^{-1} Aldrich) degradation.

RESULTS AND DISCUSSION

The crystalline phases of the prepared Ag@AgCl photocatalyst were determined, and the XRD pattern obtained is shown in Figure 1. The X-ray diffraction pattern clearly indicated the

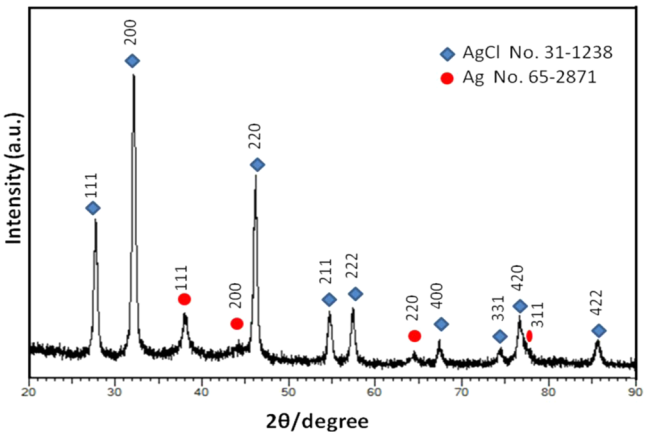

Figure 1. XRD pattern of as-synthesized Ag@AgCl.

presence of two phases, i.e., Ag and AgCl, because the obtained XRD pattern matches the JCPDS file 65-2871 for cubic Ag metal and JCPDS file 31-1238 for AgCl solid. The XRD pattern can be indexed according to the 2θ values for silver and silver chloride as shown in Figure 1.

The peaks at 2θ values 27.9, 32.3, 46.3, 54.9, 57.5, 67.2, 74.6, 76.8, and 85.9 can be assigned to (111), (200), (220), (311), (222), (400), (331), (420), and (422) planes of AgCl, respectively. The peaks at 2θ values 37.83, 44.01, 64.24, and 77.48 can be assigned to (111), (200), (220), and (311) planes of silver, respectively. The average crystallite size determined by using the Debye−Scherrer equation $Dv = K\lambda/\beta \cos\theta$ (where D_v is the average crystalline size, λ is the wavelength of Cu Kα, β is the full width at half-maximum of the diffraction peaks, and θ is the Bragg's angle) was found to be 37 nm. This showed that almost all NPs have sizes less than 50 nm, leading to the availability of high surface area for catalytic activity.

The transmission electron microscopy (TEM) image of Ag@AgCl is shown in Figure 2.

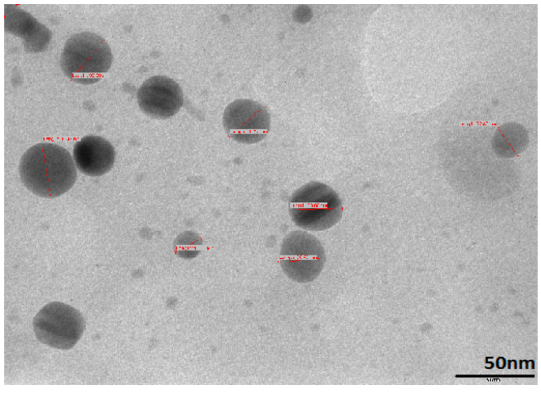

Figure 2. TEM image of Ag@AgCl NPs.

The TEM image of Ag@AgCl NPs was used to study the size and morphological features of synthesized Ag@AgCl NPs. Figure 2 clearly indicates that NPs are uniform in size with particle sizes less than 50 nm. This is in accordance with the average crystallite size obtained by using the Debye−Scherrer equation. The image also exhibits that the NPs of Ag@AgCl are well dispersed and are not aggregated. The TEM image indicated that the NPs of Ag@AgCl with particle sizes less than 10 nm were also present along with particles of an average size of 37 nm. The elemental composition of the prepared Ag@AgCl NPs was confirmed by XPS and EDS. The chemical compositions of the Ag@AgCl were characterized by X-ray photoelectron spectroscopy (XPS), as shown in Figure 3.

The survey scan spectrum in Figure 3a indicates that the sample consists of Ag and Cl as major elements, besides small amounts of O and C. The small amounts of the Ag metal species are probably at irregular intervals embedded among the AgCl matrix, and the surface analytic method XPS cannot easily gather enough signals belonging to the Ag metal species. The C 1s and O 1s peaks are attributed to a trace amount of juice molecules adsorbed on the surfaces of the NPs. The Ag 3d spectrum consists of two peaks at about 376.3 and 370.2 eV, which correspond to the binding energies of Ag $3d_{3/2}$ and Ag $3d_{5/2}$, respectively, with a doublet separation of D = 6.1 eV (Figure 3b). In addition, two peaks at about 200.1 and about 198.4 eV appear in the Cl 2p spectrum (Figure 3c), corresponding to the binding energies of Cl $2p_{1/2}$ and Cl $2p_{3/2}$, respectively, with a doublet separation of 1.7 eV. All these XPS spectra match well with the literature data[27,11] as well as with recorded EDS (Figure 4b). The recorded EDS spectrum and SAED pattern of the prepared Ag@AgCl is shown in Figure 4a and b, respectively.

This clearly indicates the presence of Ag and Cl in the composition. The SAED pattern shown in Figure 4a also confirms that the material is highly crystalline and supports the unit cell structure of Ag and AgCl.

The effect of the amount of juice, temperature, and concentration on the formation of Ag@AgCl conditions were optimized as follows:

The amount of silver nitrate was kept constant (1.5 mmol), and the amount of sugar cane juice was varied as 10, 20, 25, and 30 mL to understand the role of sugar cane juice. In a typical synthesis, 1.5 mmol (254.80 mg) of $AgNO_3$ was dissolved in the respective amount of sugar cane juice in a 50 mL round-bottomed flask, which resulted in formation of pale yellow-colored turbidity just after mixing. The whole mixture was vigorously stirred on a hot plate at a temperature of 80 °C for 20 min. After 20 min, the obtained NPs were separated as per the procedure described in the Experimental section of synthesis of Ag@AgCl. The FEG-SEM image at 10 mL of juice and TEM images at 20, 25, and 30 mL of juice of the obtained Ag@AgCl NPs are shown in Figure 5.

The TEM images revealed that the sugar cane juice plays a crucial role in deciding the morphology and dispersion of Ag@AgCl NPs. At 10 mL, the NPs were not uniform in size or shape and were not well dispersed, but at 20 and 25 mL, they are uniform in size and dispersion was enhanced. At 30 mL of sugar cane juice, the obtained Ag@AgCl NPs are highly uniform in size and shape and also well dispersed with no aggregation. The molar ratios of the obtained Ag:AgCl were found to be different with 20, 25, and 30 mL of juice (Table S2, Supporting Information). Thus, at low concentration of juice, only reduction occurs, but as we increase the amount of juice,

dx.doi.org/10.1021/sc4005668 | ACS Sustainable Chem. Eng. 2014, 2, 1007−1013

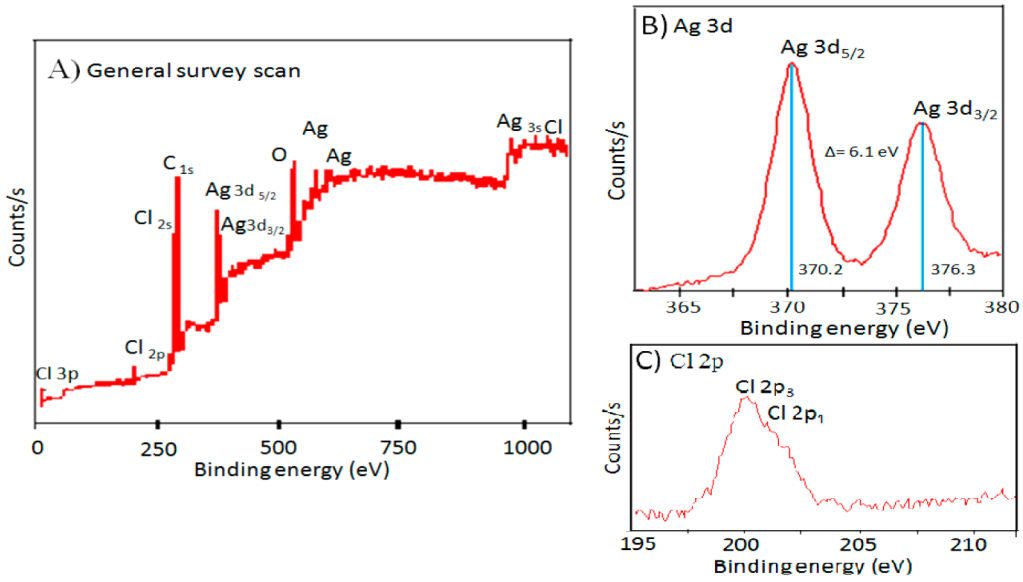

Figure 3. XPS spectra of Ag/AgCl (A) survey scan, (B) Ag 3d, and (C) Cl 2p.

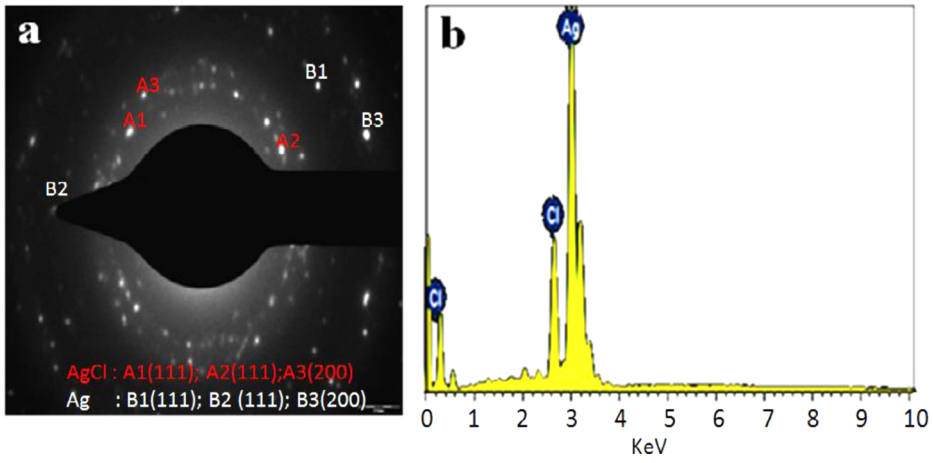

Figure 4. (a) SAED pattern and (b) EDS spectrum of Ag@AgCl photocatalyst.

the juice also serves as a capping agent to avoid aggregation of NPs.

Aiming for high catalytic activity for degradation of dyes, the amounts of juice (30 mL) and silver nitrate (1.5 mmol) were fixed. To study the effect of temperature, the reactions were conducted at 40, 60, and 80 °C. No reaction occurs at 40 and 50 °C (confirmed by XRD); the product obtained at 60 °C was Ag@AgCl. The SEM image is shown in Figure 6. The FEG-SEM image shows high aggregation of NPs, which causes them to provide less surface area for catalytic application.

The Ag@AgCl NPs obtained at 80 °C were well dispersed, which leads to availability of a high surface area causing degradation of dyes in less time. No reaction occurs within 15 min as confirmed by XRD and EDS of obtained products with an interval of 5 min (also can be easily recognized by no change in color). After 20 min, the reaction is completed (easily observed by the change in color of the solution from grayish and then black), providing a good yield of Ag@AgCl NPs that are highly uniform in size and shape, well dispersed, and stable for a longer time.

A plausible mechanism for the formation of Ag@AgCl was proposed on the basis of observations made during the synthesis. When $AgNO_3$ was mixed with sugar cane juice, instantly a precipitate was formed that appeared pale yellow because of the intrusive sugar cane juice color. The precipitate was separated and analyzed by XRD, which confirm the formation of AgCl only. This confirms that first step is the formation of AgCl by the combination of the silver ion from the metal precursor and the chloride ion from the sugar cane juice. The AgCl is sparingly soluble salt, and its solubility in water at room temperature is 1.9×10^{-6} mol L^{-1}, which increases slightly at higher temperature. The AgCl formed is surrounded by an organic capping agent present naturally in juice in its composition. Thus, juice serves both as the chloride ion-supplying agent and also as a mixture of capping agent that is naturally available. Once the solution containing AgCl formed at room temperature was allowed to heat at 80 °C, its solubility increases in water providing silver ions and some chloride ions by the reversible reaction. These silver ions are reduced to metallic silver by the reducing sugars present in the juice. As the concentration of silver ions after reduction decreases, the equilibrium is shifted again in the forward direction according to Le Chatelier's principle. To check the capping action of the chemicals naturally present in the juice and verify the predicted

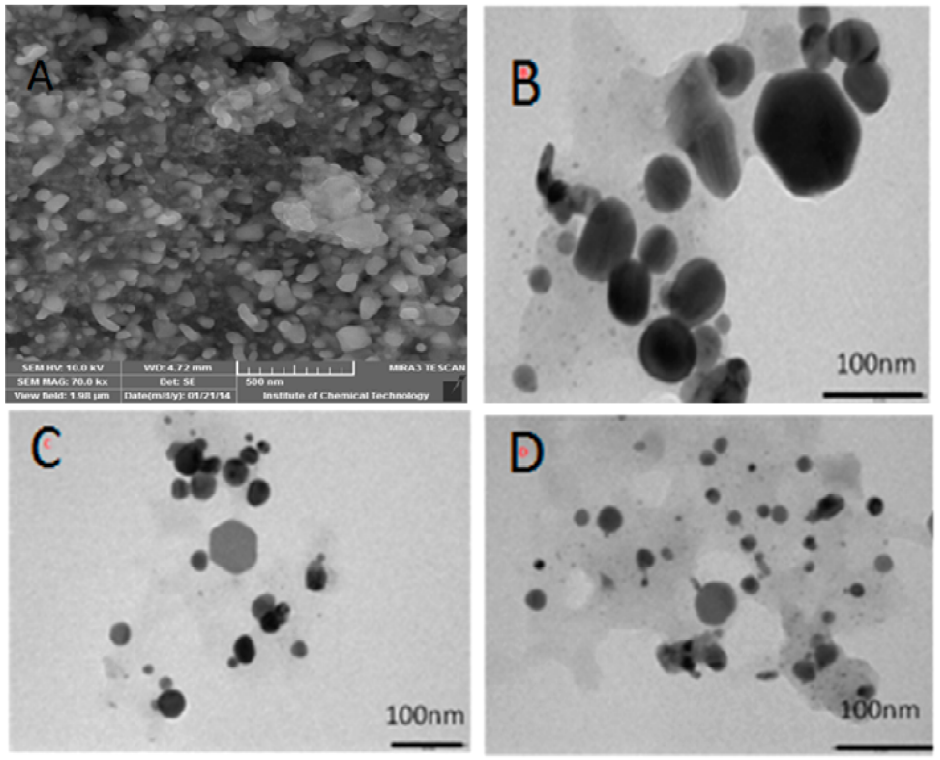

Figure 5. (A)FEG-SEM image of Ag@AgCl for 10 mL sugar cane juice. TEM images of Ag@AgCl using (B) 20 mL, (C) 25 mL, and (D) 30 mL of sugar cane juice.

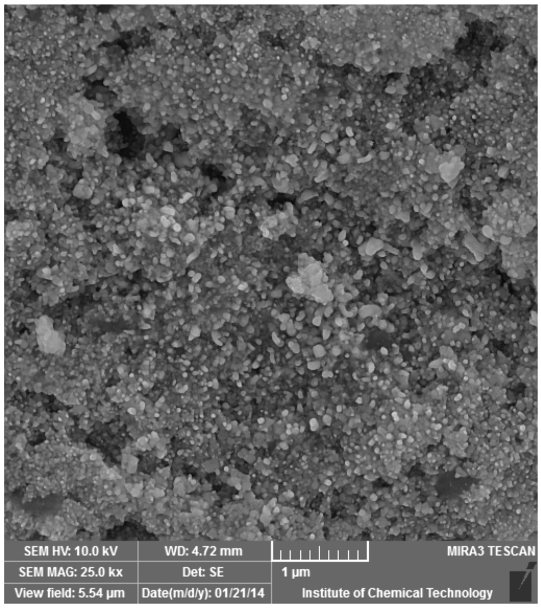

Figure 6. FEG-SEM image of Ag@AgCl at 60 °C.

mechanism, a controlled experiment of the same amount of $AgNO_3$ (254.80 mg) with 264.9 mg of A.R grade glucose and 12 mg of A.R grade NaCl (stoichiometry calculations were made as per the glucose and chloride ion present in the analyzed juice sample and amount of juice used) was performed under the same experimental conditions (given under synthesis of Ag@AgCl). We observed that the obtained Ag@AgCl NPs have sizes from 0.40 to 0.50 μm (Figure S1, Supporting Information). This experiment clearly indicated that the chemicals in sugar juice can pin down the growth of Ag@AgCl NPs, which was not observed by using pure glucose as the reducing agent in nanoparticle synthesis.

Thus, when visible light falls on the catalyst, the Ag metal NPs on the AgCl undergoes surface plasmon resonance (SPR) that causes the excitation and subsequent transfer of electrons to the conduction band of AgCl NPs attached to it, leading to photocatalytic activity of the AgCl catalyst to work under visible light. In the absence of plasmonic Ag NPs, the AgCl does not shows any photocatalytic activity in visible light because of its huge band gap that makes it unable to absorb in the visible region of light.

The resultant Ag@AgCl NPs were tested for the study of photocatalytic activity for the degradation of MO dye and MB dye. The UV spectra obtained for the samples removed after an equal interval of time are shown in Figures 7 and 8, respectively.

The MO dye absorbs in the visible region of light at 464 nm (Figure 7), and the intensity of the absorption peaks decreases as the reaction times proceed. The samples are collected after 0, 3, 6, 9, 12, and 18 min. The recorded UV spectra clearly indicate the successive decrease in absorption maximum, and within almost 21 min, all the MO dye is completely degraded (Figure S2, Supporting Information). Such a short time for degradation is needed because the small size of the Ag@AgCl NPs provide their large surface area for degradation of the methyl orange dye. To extend the application of the catalyst to other dyes, the degradation of MB was also studied, which also absorbs in the visible region of light at 667 nm as shown in Figure 8. The degradation reaction was also monitored by recording the UV spectrum of the reaction mixture, which was made free from catalyst by centrifugation. The obtained series of UV absorption spectra are shown in Figure 8.

dx.doi.org/10.1021/sc4005668 | ACS Sustainable Chem. Eng. 2014, 2, 1007−1013

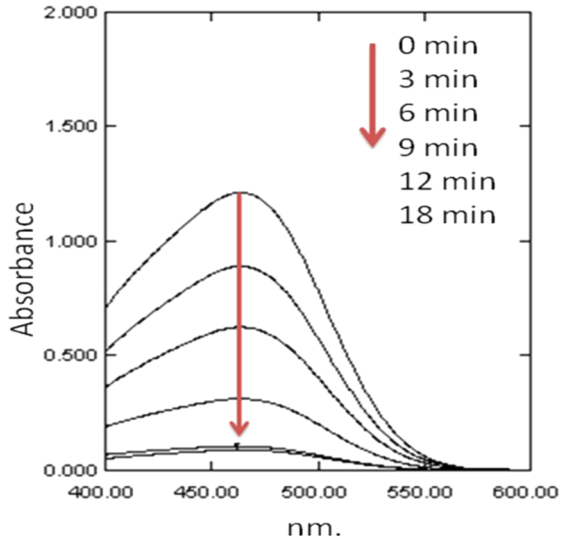

Figure 7. Series of UV spectrum of MO dye degradation at different intervals of time.

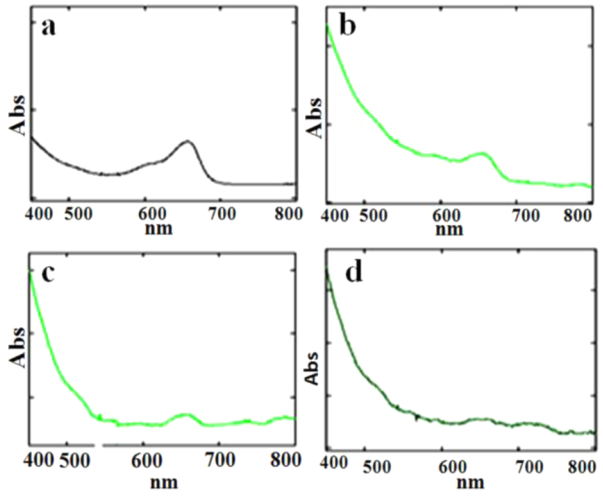

Figure 8. UV spectra for degradation of MB dye after (a) 0 min, (b) 10 min, (c) 20 min, and (d) 40 min.

The samples were collected after 10 min intervals of time. The peak at 667 nm decreases as time proceeds and almost becomes zero after 50 min, which clearly indicates that the small-sized NPs are helping with the efficient catalytic activity for the degradation of the MB dye. The MB and MO dye molecules might be degraded because of the oxidation with oxidative species such as the Cl atom from silver chloride and oxygen radicals that are formed because of the reduction of oxygen of solution by the Ag plasmonic NPs.[33,34] After each experiment, the catalyst was recovered by centrifugation, washed with ethanol, and used for the next dye degradation experiments. The catalyst actively shows recyclability of four times. The stability of the catalyst was confirmed by recording the XRD of the recyclable catalyst (Figure S3A and B, Supporting Information), and after the fourth recycled activity, the catalyst decreases notably.

CONCLUSION

A green, fast, low-temperature, and additive-free (solvents, capping agents, templates) method has been developed for the synthesis of Ag@AgCl NPs employing sugar cane juice as the multifunctional reagent. The prepared NPs are less than 50 nm (average size 37 nm and discerned particles less than 10 nm) and are stable. Ag@AgCl NPs have been found to be highly efficient photocatalysts for rapid degradation of MO and MB azo dyes.

ASSOCIATED CONTENT

Supporting Information

Characterization data of the composition of sugar juice, molar ratio of prepared Ag:AgCl with different volumes of juice, structure of Ag@AgCl prepared by using pure glucose, and recyclability of the catalyst. This material is available free of charge via the Internet at http://pubs.acs.org.

AUTHOR INFORMATION

Corresponding Author

* Tel.: + 91- 22 3361 1111/2222. Fax: +91- 22 2414 5614. E-mail: bm.bhanage@gmail.com, bm.bhanage@ictmumbai.edu.in.

Notes

The authors declare no competing financial interest.

ACKNOWLEDGMENTS

The authors express their gratitude toward the Department of Science and Technology (DST), India, for providing financial assistance as an INSPIRE fellowship. We gratefully acknowledge the financial assistance from the Department of Science and Technology (DST), India, under the Nano Mission Project (No. SR/NM/NS-1097/2011). We are also thankful to Dr. P. P Wadgaonkar (CSIR-NCL Pune) for providing the XPS analysis facility.

REFERENCES

(1) Goodsell, D. S. Bionanomedicine in Action. In *Bionanotechnology: Lessons from Nature*; John Wiley & Sons, Inc.: Hoboken, NJ, 2004.

(2) Husseiny, M. I.; El-Aziz, M. A.; Badr, Y.; Mahmoud, M. A. Biosynthesis of gold nanoparticles using *Pseudomonas aeruginosa*. *Spectrochim. Acta, Part A* **2007**, *67* (3−4), 1003−1006.

(3) Mukherjee, P.; Ahmad, A.; Mandal, D.; Senapati, S.; Sainkar, S. R.; Khan, M. I.; Ramani, R.; Parischa, R.; Ajaykumar, P. A.; Alam, M.; Sastry, M.; Kumar, R. Bioreduction of $AuCl_4^-$ ions by the fungus,Verticillium sp. and surface trapping of the gold nanoparticles formed. *Angew Chem, Int. Ed.* **2001b**, *40* (19), 3585−3588.

(4) Sastry, M.; Ahmad, A.; Khan, M. I.; Kumar, R. Biosynthesis of metal nanoparticles using fungi and actinomycete. *Curr. Sci.* **2003**, *85* (2), 162−170.

(5) Kowshik, M.; Arhtaputre, S.; Kharrazi, S.; Vogel, W.; Urban, J.; Kulkarni, S. K.; Paknikar, K. M. Extracellular synthesis of silver nanoparticles by a silver-tolerant yeast strain MKY3. *Nanotechnology* **2003**, *14*, 95−100.

(6) Lee, S. W.; Mao, C.; Flynn, C.; Belcher, A. M. Ordering of quantum dots using genetically engineered viruses. *Science* **2002**, *296*, 892−895.

(7) Akhtar, M. S.; Panwar, J.; Yun, Y. S. Biogenic synthesis of metallic nanoparticles by plant extracts. *ACS Sustainable Chem. Eng.* **2013**, *1*, 591−602.

(8) Oxana, V.; Kharissova1, H. V.; Dias, R.; Boris, I.; Kharisov; Perez, B. O.; Victor, M.; Jimenez, P. The greener synthesis of nanoparticles. *Trends Biotechnol.* **2013**, *31*, 4.

(9) Mittala, A. K.; Chistib, Y.; Banerjeea, U. C. *Biotechnology Adv.* **2013**, *31*, 346−356.

(10) Shankar, S. S.; Rai, A.; Ahmad, A.; Sastry, M. Rapid synthesis of Au, Ag, and bimetallic Au core−Ag shell nanoparticles using neem (*Azadirachta indica*) leaf broth. *J. Colloid Interface Sci.* **2004a**, *275* (2), 496−502.

(11) Thai, C. C. D.; Doherty, W. O. S. Characterisation of Sugarcane Juice Particles That Influence the Clarification Process. In *Proceedings of the Australian Society of Sugar Cane Technologists*; Cairns, Queensland, Australia; Bruce, R., Ed.; 2012; http://eprints.qut.edu.au/.
(12) Fort, C. A.; McKaig, N. Comparative Chemical Composition of Juices of Different Varieties of Louisiana Sugarcane; Technical Bulletin 688; United States Department of Agriculture: Washington, DC, 1939.
(13) Thai, C. C. D.; Doherty, W. O. S. In *33rd Annual Conference of the Australian Society of Sugar Cane Technologists 2011*; Bruce, R., Ed.; Curran Associates, Inc.: Mackay, Queensland, Australia, 2011; p 368.
(14) Hoffmann, M. R.; Martin, S. T.; Choi, W. Y.; Bahnemann, D. W. Environmental applications of semiconductor photocatalysis. *Chem. Rev.* **1995**, *95*, 69−96.
(15) Wu, C. G.; Chao, C. C.; Kuo, F. T. Enhancement of the photo catalytic performance of TiO_2 catalysts via transition metal modification. *Catal. Today* **2004**, *97*, 103−112.
(16) Tachikawa, T.; Tojo, S.; Kawai, K.; Endo, M.; Fujitsuka, M.; Ohno, T.; Nishijima, K.; Miyamoto, Z.; Majima, T. Photocatalytic oxidation reactivity of holes in the sulfur and carbon-doped TiO_2 powders studied by time-resolved diffuse reflectance spectroscopy. *J. Phys. Chem. B* **2004**, *108*, 19299−19306.
(17) Bae, E.; Choi, W.; Park, J.; Shin, H. S.; Kim, S. B.; Lee, J. S. Effects of surface anchoring groups (carboxylate vs phosphonate) in ruthenium-complex-sensitized TiO_2 on visible light reactivity in aqueous suspensions. *J. Phys. Chem. B* **2004**, *108*, 14093−14101.
(18) Kou, J.; Varma, R. S. Beet juice-induced green fabrication of plasmonic AgCl/Ag nanoparticles. *ChemSusChem.* **2012**, *5*, 2435−2441.
(19) An, C.; Peng, S.; Sun, Y. Facile synthesis of sunlight-driven AgCl:Ag plasmonic nanophotocatalyst. *Adv. Mater.* **2010**, *22*, 2570−2574.
(20) Kou, J. H.; Gao, J.; Li, Z. S.; Zou, Z. G. Research on photocatalytic degradation properties of organics with different new photocatalysts. *Curr. Org. Chem.* **2010**, *14*, 728−744.
(21) Chen, C.; Ma, W.; Zhao, J. Semiconductor-mediated photodegradation of pollutants under visible-light irradiation. *Chem. Soc. Rev.* **2010**, *39*, 4206−4219.
(22) Huang, W. Y.; Yu, Y. Development of visible-light activated titanium dioxide films with femtosecond laser. *Prog. Chem.* **2005**, *17*, 242−247.
(23) Wang, P.; Huang, B.; Lou, Z.; Zhang, X.; Qin, X.; Dai, Y.; Zheng, Z.; Wang, X. Synthesis of highly efficient Ag@AgCl plasmonic photocatalysts with various structures. *Chem.—Eur. J.* **2010**, *16*, 538−544.
(24) Wang, P.; Huang, B.; Zhang, Q.; Zhang, X.; Qin, X.; Dai, Y.; Zhan, J.; Yu, J.; Liu, H.; Lou, Z. Highly efficient visible light plasmonic photocatalyst Ag@Ag(Br,I). *Chem.—Eur. J.* **2010**, *16*, 10042−10047.
(25) Wang, P.; Huang, B.; Zhang, X.; Qin, X.; Dai, Y.; Wang, Z.; Lou, Z. Highly efficient visible light plasmonic photocatalysts Ag@Ag(Cl,Br) and Ag@AgCl-AgI. *ChemCatChem.* **2011**, *3*, 360−364.
(26) Wang, P.; Huang, B.; Qin, X.; Zhang, X.; Dai, Y.; Wei, J.; Whangbo, M. H. Ag@AgCl: A highly efficient and stable photocatalyst active under visible light. *Angew. Chem.* **2008**, *120*, 8049−8051.
(27) Chen, D.; Yoo, S. H.; Huang, Q.; Ali, G.; Cho, S. O. Sonochemical synthesis of Ag/AgCl nanocubes and their efficient visible-light-driven photocatalytic performance. *Chem.—Eur. J.* **2012**, *18*, 5192−5200.
(28) Bi, Y.; Ye, J. In situ oxidation synthesis of Ag/AgCl core−shell nanowires and their photocatalytic properties. *Chem. Commun.* **2009**, 6551−6553.
(29) Lou, Z.; Huang, B.; Wang, P.; Wang, Z.; Qin, X.; Zhang, X.; Cheng, H.; Zheng, Z.; Dai, Y. The synthesis of the near-spherical AgCl crystal for visible light photocatalytic applications. *Dalton Trans.* **2011**, *40*, 4104−4110.
(30) Xu, H.; Li, H.; Xia, J.; Yin, S.; Luo, Z.; Liu, L.; Xu, L. One-pot synthesis of visible-light-driven plasmonic photocatalyst Ag/AgCl in Ionic Liquid. *ACS Appl. Mater. Interfaces* **2011**, *3*, 22−29.
(31) Song, J.; Roh, J.; Lee, I.; Jang, J. Low temperature aqueous phase synthesis of silver/silver chloride plasmonic nanoparticles as visible light photocatalysts. *Dalton Trans.* **2013**, *42*, 13897.
(32) Tang, Y.; Jiang, Z.; Xing, G.; Li, A.; Kanhere, P. D.; Zhang, Y.; Sum, T. C.; Li, S.; Chen, X.; Dong, Z.; Chen, Z. Efficient Ag@AgCl cubic cage photocatalysts profit from ultrafast plasmon-Induced electron transfer processes. *Adv. Funct. Mater.* **2013**, *23*, 2932−2940.
(33) Houas, A.; Lachheb, H.; Ksibi, M.; Elaloui, E.; Guillard, C.; Herrmann, J. M. Photocatalytic degradation pathway of methylene blue in water. *Appl. Catal., B* **2001**, *31*, 145−157.
(34) Comparelli, R.; Fanizza, E.; Curri, M. L.; Cozzoli, P. D.; Mascolo, G.; Agostiano, A. UV-induced photocatalytic degradation of azo dyes by organic-capped ZnO nanocrystals immobilized onto substrates. *Appl. Catal., B* **2005**, *60*, 1−11.